*Neural Processing Letters* **20:** 71–83, 2004.



# Neuronal Signal Transduction Aided by Noise at Threshold and at Saturation

DAVID ROUSSEAU and FRANÇOIS CHAPEAU-BLONDEAU*
*Laboratoire d'Ingénierie des Systèmes Automatisés (LISA), Université d'Angers, 62 avenue Notre Dame du Lac, 49000 Angers, France. e-mail: chapeau@univ-angers.fr*

**Abstract.** A classical model of neuronal signal transmission describing the presence of both a threshold and a saturation in the neuron response is considered. This model is used to analyze the transduction by the neuron of various types of information-carrying input signals in the presence of noise. Improvement by noise of the performance via stochastic resonance is established for transmission in both the threshold and the saturation regimes. Stochastic resonance at saturation is a novel form, expressing that the distortion experienced by large input signals transmitted at saturation, can be reduced by addition of noise.

**Key words.** neuronal transmission, noise, saturation, stochastic resonance, threshold

## 1. Introduction

Stochastic resonance is a phenomenon which expresses the possibility of improving the transmission of a signal by certain nonlinear systems, thanks to addition of noise [1]. This paradoxical effect was introduced some 20 years ago in the context of geophysical dynamics, and it has subsequently been observed in a growing variety of processes, including electronic circuits, optical devices or chemical reactions. Neurons constitute an important class of nonlinear systems that have been shown to lend themselves to stochastic resonance. Various forms of neuronal signal transmission aided by noise have been shown feasible, both in theoretical models [2–4] and in experimental preparations [5–8].

So far, systems that were proven capable of stochastic resonance, essentially are nonlinear systems with potential barriers or with thresholds. In such conditions, the essence of the effect is that the information-carrying signal by itself is too small to overcome a threshold or a barrier in the response of the system. Addition of noise then allows some type of cooperation between the signal and the noise, so as to overcome a threshold or barrier, and to elicit a response bearing stronger relation to the signal thanks to assistance from the noise. These circumstances apply for neuronal signal transmission aided by noise. It is essentially in the region of the neuron threshold, or sensitivity threshold, that it has been demonstrated that the transmission of small subthreshold signals can be improved by the action of the noise.

* corresponding author.

In the present report, we shall establish that stochastic resonance, or noise-improved signal transmission, can also occur in the region of the saturation of the neuronal response. Large signals transmitted by a saturating nonlinearity can experience strong distortion in their transmission. Addition of noise can reduce this distortion. This possibility was recently demonstrated in simple models of saturating nonlinearities [9]. Here, we shall demonstrate that this possibility is also authorized in a model of neuronal transmission which incorporates saturation in the response. This is a novel form of stochastic resonance which is established for neuronal transmission of large signals in the saturation region. The classical model of neuronal transmission we consider, also incorporates the threshold in the response, in addition to the saturation. It allows us to establish, with the same model of neuronal transmission, that addition of noise can improve the performance for both small signals below threshold as well as for large signals in the saturation. For a standard neuronal response, with threshold and saturation, our results express that noise can broaden the operating dynamic range of the neuron, from both ends.

## 2. The Model of Neuronal Signal Transmission

We consider a model of neuronal signal transmission in which the input signal to the neuron, at time $t$, is taken as the total somatic current $I(t)$. This electric current $I(t)$ results from the gating of ion channels in the neuronal membrane, trigged by synaptic inputs or by physical stimuli from the environment for sensory neurons. The output response of the neuron is taken as the short-term firing rate $f(t)$ at which action potentials are emitted in response to $I(t)$. A classical modeling of the integrate-and-fire dynamics of the neuron, allows one to deduce an input–output firing function $g(.)$, under the so-called Lapicque form [10, 11]

$$f(t) = g[I(t)] = \begin{cases} 0 & \text{for} \quad I(t) \leq I_{\text{th}}, \\ \dfrac{1/T_{\text{r}}}{1-(\tau_{\text{m}}/T_{\text{r}})\ln[1-I_{\text{th}}/I(t)]} & \text{for} \quad I(t) > I_{\text{th}}. \end{cases} \tag{1}$$

In the firing function of Equation (1), a threshold current is introduced as $I_{\text{th}} = V_{\text{th}}/R_{\text{m}}$ with $V_{\text{th}}$ the standard firing potential of the neuron, and $R_{\text{m}}$ its total membrane resistance. Also in Equation (1), $\tau_{\text{m}}$ is the membrane time constant, and $T_{\text{r}}$ the neuron refractory period. Typically $V_{\text{th}} \approx 10$ mV above the neuron resting potential, and as an order of magnitude $R_{\text{m}} \approx 100$ MΩ; this leads to a current threshold of order $I_{\text{th}} \approx 0.1$ nA. Other orders of magnitude are $\tau_{\text{m}} \approx 10$ ms and $T_{\text{r}} \approx 1$ ms. The neuron firing function of Equation (1) is depicted in Figure 1.

Although resulting from a very simplified description of the neuronal dynamics, the firing function of Equation (1) is able to capture essential features of the neuron response [10, 11]. As visible in Figure 1, the firing function of Equation (1) describes the important qualitative properties of the existence of a threshold, at low input, and of a saturation, at large input, in the neuron response. Furthermore, at a quantitative level, Figure 1 shows the necessity of several decades (approximately three to five) of variation in the input variable $I(t)$, in order to make an effective use of the whole

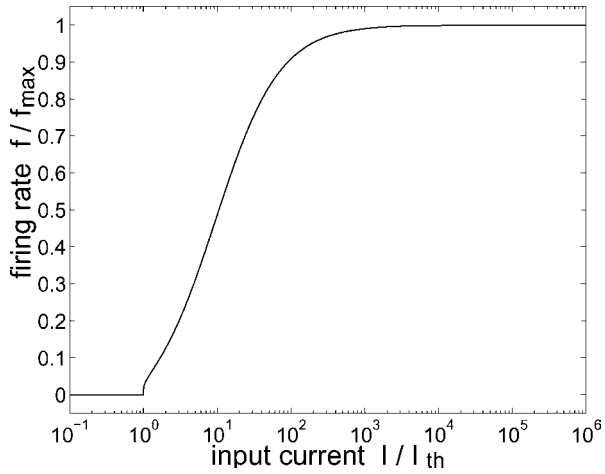


*Figure 1.* Output firing rate $f(t)$ in units of $f_{\max} = 1/T_r$, as a function of the input somatic current $I(t)$ in units of $I_{th}$, according to the neuron firing function of Equation (1), in typical conditions with $\tau_m = 10$ ms, $T_r = 1$ ms and $I_{th} = 0.1$ nA.

range of the response curve, from the subthreshold region up to the saturation through the curvilinear part. The curvilinear part of the response, above threshold and before saturation, is covered roughly by three decades of variation; an additional decade can be used to operate the neuron below threshold for subthreshold dynamics, symmetrically an additional decade will operate the neuron in the saturation region. These several decades of input variation can be related to the range of several decades in the number of active synaptic inputs that a typical neuron may receive. These several decades of input variation can also be related to the large dynamics available to most sensory modalities, from vision to hearing, to touch.[1] Our main point is to express that it is quite plausible, for a typical neuron, to have to operate, in normal operating conditions, over the whole range of the response curve of Figure 1, including the threshold and the saturation regions. We shall then show that, both in the threshold and in the saturation regions, but not in the curvilinear part in-between, noise can benefit to signal transmission by the neuron.

## 3. Assessing Nonlinear Signal Transmission

To demonstrate a neuronal transmission aided by noise, we consider that the input current $I(t)$ to the neuron is formed as

$$I(t) = s(t) + \eta(t). \tag{2}$$

In Equation (2), $s(t)$ is our information-carrying signal, which will be successively considered to be a periodic and an aperiodic component. $s(t)$ conveys an image of the

[1] Vision is sensitive to light over several decades of luminance. Normal hearing operates over at least, a 100 dB range in acoustic pressure. Touch can accomodate stimuli from below a few grams to several kilograms.

information coming from presynaptic neurons or from the physical world for sensory cells. Also in Equation (2), $\eta(t)$ is a white noise, independent of $s(t)$, with a probability density function $p_\eta(u)$. This noise $\eta(t)$ may have its origin in random gating of the ion channels of the membrane, or in random activities of presynaptic neurons, or in the physical world.

The input signal-plus-noise mixture $I(t) = s(t) + \eta(t)$ is transmitted by the neuron nonlinearity $g(.)$ of Equation (1), so as to produce the output signal

$$f(t) = g[s(t) + \eta(t)]. \tag{3}$$

We shall now apply techniques from stochastic resonance theory, in order to quantify how the output firing rate $f(t)$ is related to the information-carrying input $s(t)$. We shall show that, depending of the conditions of operation of the nonlinearity $g(.)$ in Equation (3), regimes exist where enhancement of the noise $\eta(t)$ can result in improved transmission of $s(t)$ onto $f(t)$, i.e. stoehastic resonance.

### 3.1. PERIODIC SIGNAL TRANSMISSION

In the case of a periodic information-carrying signal $s(t)$, the standard measure of stochastic resonance is a signal-to-noise ratio, defined in the frequency domain, and which measures, in the output signal, the part contributed by the periodic input and the part contributed by the noise [1, 12]. When $s(t)$ in Equation (2) is deterministic periodic with period $T_s$, the output signal $f(t)$ of Equation (3) generally is a cyclostationary random signal, with a power spectrum containing spectral lines at integer multiples of $1/T_s$ emerging out of a continuous noise background [12]. A standard measure of similarity of $f(t)$ with the $T_s$-periodic input $s(t)$, is a signal-to-noise ratio defined as the power contained in the output spectral line at the fundamental $1/T_s$ divided by the power contained in the noise background in a small frequency band $\Delta B$ around $1/T_s$.

For the input–output relationship of Equation (3). the power contained in the output spectral line at the frequency $n/T_s$ is given [12] by $|\overline{F}_n|^2$ where $\overline{F}_n$ is the order $n$ Fourier coefficient of the $T_s$-periodic nonstationary output expectation $\mathrm{E}[f(t)]$, i.e.,

$$\overline{F}_n = \left\langle \mathrm{E}[f(t)] \exp\left(-in\frac{2\pi}{T_s}t\right)\right\rangle, \tag{4}$$

with the time average defined as

$$\langle ... \rangle = \frac{1}{T_s}\int_0^{T_s} ... \mathrm{d}t. \tag{5}$$

The output expectation $\mathrm{E}[f(t)]$ at a fixed time $t$ is computable as

$$\mathrm{E}[f(t)] = \int_{-\infty}^{+\infty} g(u) p_\eta[u - s(t)] \mathrm{d}u. \tag{6}$$

The magnitude of the continuous noise background in the output spectrum is measured [12] by the stationarized output variance $\langle \mathrm{var}[f(t)] \rangle$, with the nonstationary variance $\mathrm{var}[f(t)] = \mathrm{E}[f^2(t)] - \mathrm{E}[f(t)]^2$ at a fixed time $t$, and

$$\mathrm{E}[f^2(t)] = \int_{-\infty}^{+\infty} g^2(u) p_\eta[u - s(t)] \mathrm{d}u. \tag{7}$$

A signal-to-noise ratio $\mathcal{R}_n$, for the harmonic $n/T_s$ in the output $f(t)$, follows as

$$\mathcal{R}_n = \frac{|\overline{F}_n|^2}{\langle \mathrm{var}[f(t)] \rangle \Delta t \Delta B}, \tag{8}$$

where $\Delta t$ is the time resolution of the measurement (i.e., the signal sampling period in a discrete-time implementation).

In practice, an expectation like E[.] in Equations (6) or (7) expresses an average which is performed over independent realizations of the noise $\eta(t)$ in presence of the same signal $s(t)$. The average of Equation (5) denotes an average over one temporal period $T_s$ of $s(t)$, i.e. over all time configurations of the input periodic waveform. The signal-to-noise ratio $\mathcal{R}_n$ of Equation (8) therefore quantifies the average performance of the transmission of $s(t)$ onto $f(t)$, both averaged in time over one period $T_s$ and averaged according to the noise realizations. In addition to the theoretical expression of $\mathcal{R}_n$ of Equation (8), many practical calculations of $\mathcal{R}_n$ from observed data have appeared, and specially in the context of neuronal signals to characterize periodic stochastic resonance [5, 8].

### 3.2. APERIODIC SIGNAL TRANSMISSION

When the information-carrying input signal $s(t)$ we seek to extract out of the output rate $f(t)$ is no longer periodic, then the signal-to-noise ratio $\mathcal{R}_n$ of Equation (8) is no longer available as a meaningful input–output measure of similarity. Consider $s(t)$ a deterministic aperiodic signal existing over the duration $T_s$. In such a case, meaningful input-output measures of similarity are provided by cross-correlations as used for instance in [13, 14]. We choose here to use the normalized time-averaged cross-covariance between input $s(t)$ and output $f(t)$; it provides a similarity measure insensitive to both scaling and translation in signal amplitude. We introduce the signals centered around their time-averaged statistical expectation,

$$\widetilde{s}(t) = s(t) - \langle s(t) \rangle \tag{9}$$

and

$$\widetilde{f}(t) = f(t) - \langle \mathrm{E}[f(t)] \rangle, \tag{10}$$

with the time average again defined by Equation (5). The normalized time-averaged cross-covariance is

$$C_{sf} = \frac{\langle \mathrm{E}[\widetilde{s}(t)\widetilde{f}(t)] \rangle}{\sqrt{\langle \mathrm{E}[\widetilde{s}^2(t)] \rangle \langle \mathrm{E}[\widetilde{f}^2(t)] \rangle}}, \tag{11}$$

or equivalently, since $s(t)$ is deterministic,

$$C_{sf} = \frac{\langle s(t)\mathrm{E}[f(t)] \rangle - \langle s(t) \rangle \langle \mathrm{E}[f(t)] \rangle}{\sqrt{[\langle s(t)^2 \rangle - \langle s(t) \rangle^2][\langle \mathrm{E}[f^2(t)] \rangle - \langle \mathrm{E}[f(t)] \rangle^2]}}, \tag{12}$$

with $\mathrm{E}[f(t)]$ and $\mathrm{E}^2[f(t)]$ again given by Equations (6) and (7).

In the same way as the signal-to-noise ratio $\mathcal{R}_n$ of Equation (8) for periodic $s(t)$, the cross-covariancc $C_{sf}$ of Equation (12) for aperiodic $s(t)$ is an average quantity, quantifying the average performance of the transmission, averaged both over the time waveform $s(t)$ and over the noise realizations. Also, in addition to the theoretical expression of $C_{sf}$ of Equation (12), practical calculations of $C_{sf}$ from observed data have appeared, specially for neuronal signals [13, 15].

With the measures of performance $\mathcal{R}_n$ of Equation (8) and $C_{sf}$ of Equation (12), we are now in a position to study specifically the neuronal transmission realized by Equation (1) and to show that it allows noise-aided transmission of the signal in several distinct regimes of operation.

## 4. Neuronal Transmission Aided by Noise

We shall now illustrate various possibilities of stochastic resonance in the neuronal transmission described by Equation (1). For the case of periodic signal transmission, we shall consider the information-carrying input $s(t)$ under the form

$$s(t) = I_0 + I_1 \sin(2\pi t/T_\mathrm{s}), \forall t. \tag{13}$$

In this case, we shall assess the transmission performance by means of the signal-to-noise ratio $\mathcal{R}_1$ at the fundamental frequency $1/T_\mathrm{s}$, from Equation (8) with $\Delta t \Delta B = 10^{-3}$, which measures in the output $f(t)$ how the coherent spectral line at the fundamental $1/T_\mathrm{s}$ emerges out of the noise background.

For the case of aperiodic signal transmission, we shall choose the input $s(t)$ as the transient waveform

$$s(t) = \begin{cases} I_0 + I_1 \sin(2\pi t/T_\mathrm{s}) & \text{for } t \in [0, T_\mathrm{s}], \\ 0 & \text{otherwise.} \end{cases} \tag{14}$$

In this case, we shall assess the transmission performance with the input–output normalized cross-covariance $C_{sf}$ of Equation (12), which quantifies the similarity in shape of the output rate $f(t)$ with the transient waveform $s(t)$.

The parameters $I_0$ (offset) and $I_1$ (amplitude) of the coherent input $s(t)$ of Equations (13) or (14) will be varied, in order to solicit the neuronal nonlinearity of Figure 1 in various operation ranges, successively, the threshold region, the curvilinear intermediate part, and the saturation region.

### 4.1. TRANSMISSION AT THRESHOLD

We first tune $I_0$ and $I_1$ in both Equations (13) and (14), so as to make the information-carrying input $s(t)$ a small subthreshold signal evolving always below the neuron firing threshold $I_{\text{th}}$. In this case, when the noise $\eta(t)$ is absent in Equation (2), the input current $I(t) = s(t)$ is too small to trigger any response from the neuron, and the output firing rate $f(t)$ of Equation (1) remains stuck to zero. Next, in such a situation, if we start to add some noise $\eta(t)$ in Equation (2), then a cooperative effect becomes possible, in which the noise $\eta(t)$ assists the signal $s(t)$ to overcome the threshold $I_{\text{th}}$ and trigger some output activity on $f(t)$. This activity will be correlated with the coherent input $s(t)$ which is, for a part, at its origin. It turns out that the efficacy of this cooperative effect increases as the noise level rises above zero, and it is maximized by a nonzero optimal amount of the noise $\eta(t)$. This beneficial outcome can be precisely quantified by means of the measures of performance introduced in Section 3. Figure 2A represents the output signal-to-noise ratio $\mathcal{R}_1$ from Equation (8), for the transmission of the periodic input $s(t)$ of Equation (13). Figure 2B shows the input–output normalized cross-covariance $C_{sf}$ of Equation (12). for the transmission of the aperiodic input $s(t)$ of Equation (14).

The results of Figure 2 illustrate the noise-aided signal transmission, for both the periodic and the aperiodic cases of the coherent subthreshold input $s(t)$. Both measures of performance, $\mathcal{R}_1$ of Figure 2A and $C_{sf}$ of Figure 2B, when the level of the input noise $\eta(t)$ is increased, experience nonmonotonic resonant evolutions which culminate for a nonzero optimal amount of noise. In Figure 2, because the input $s(t)$ is strictly subthreshold, the transmission efficacy measured by $\mathcal{R}_1$ and $C_{sf}$ is strictly zero at zero noise. When the rms amplitude $\sigma_\eta$ of the noise $\eta(t)$ is raised from zero, the performances $\mathcal{R}_1$ and $C_{sf}$ start to increase, and they culminate for a nonzero level of $\sigma_\eta$ (whose precise value depends on the detail of the conditions). For larger levels of $\eta(t)$, the detrimental influence of the noise progressively replaces its con-

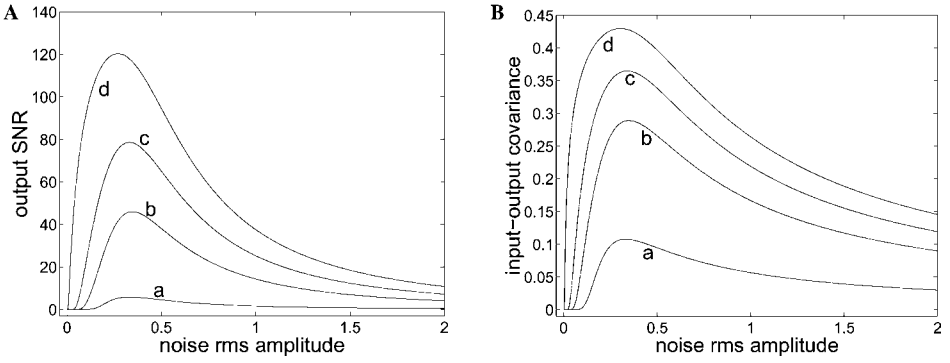


*Figure 2.* Transmission at threshold by the neuron nonlinearity of Equation (1), as a function of the rms amplitude $\sigma_\eta/I_{\text{th}}$ of the zero-mean Gaussian noise $\eta(t)$, with $I_0 = 0.5I_{\text{th}}$ and (a) $I_1 = 0.1I_{\text{th}}$ (b) $I_1 = 0.3I_{\text{th}}$ (c) $I_1 = 0.4I_{\text{th}}$ and (d) $I_1 = 0.49I_{\text{th}}$ Panel A: Output signal-to-noise ratio $\mathcal{R}_1$ from Equation (8) for the $T_s$-periodic input $s(t)$ of Equation (13). Panel B: Input–output normalized cross-covariance $C_{sf}$ of Equation (12) for the aperiodic input $s(t)$ of Equation (14).

structive action, and $\mathcal{R}_1$ and $C_{sf}$ gradually diminish, down to zero for very high noise levels. This is the stochastic resonance effect, under the form of a noise-aided transmission of a small subthreshold signal.

### 4.2. TRANSMISSION AT MEDIUM RANGE

The parameters $I_0$ and $I_1$ in both Equations (13) and (14) are now set in a medium range, neither too small nor too large, so as to make the information-carrying input $s(t)$ solicit the neuronal nonlinearity of Figure 1 in its curvilinear intermediate part, away from both the threshold and the saturation regions. In this case the input $I(t) = s(t)$, by itself, can be transmitted efficiently; it does not need assistance from the noise. If some noise $\eta(t)$ is added to $I(t)$ as in Equation (2), it is a degradation of the transmission which ensues. This is observed both for the transmission of the periodic $s(t)$ of Equation (13) and for the aperiodic $s(t)$ of Equation (14). The corresponding measures of performance, the signal-to-noise ratio $\mathcal{R}_1$ of Equation (8) and the cross-covariance $C_{sf}$ of Equation (12), are at their maximum at zero noise, and they experience monotonic decays as the noise level is raised above zero, as shown by Figure 3. No stochastic resonance occurs in this regime of transmission.

### 4.3. TRANSMISSION AT SATURATION

We now set the parameters $I_0$ and $I_1$ of Equations (13) and (14) at large values, in such a way that the information-carrying input $s(t)$ operates the neuronal nonlinearity of Figure 1 in its saturation region. The measures of performance $\mathcal{R}_1$ and $C_{sf}$ for the resulting periodic and aperiodic transmissions, are represented in Figure 4.

Figure 4 shows (except in Figure 4B(d) with very strong saturation) that when the noise is strictly zero, both performance measures $\mathcal{R}_1$ and $C_{sf}$ are at their best. This is due to the smooth character of the nonlinearity of Equation (1) in its saturation region (as opposed to the threshold region of Figure 2). A smooth response curve

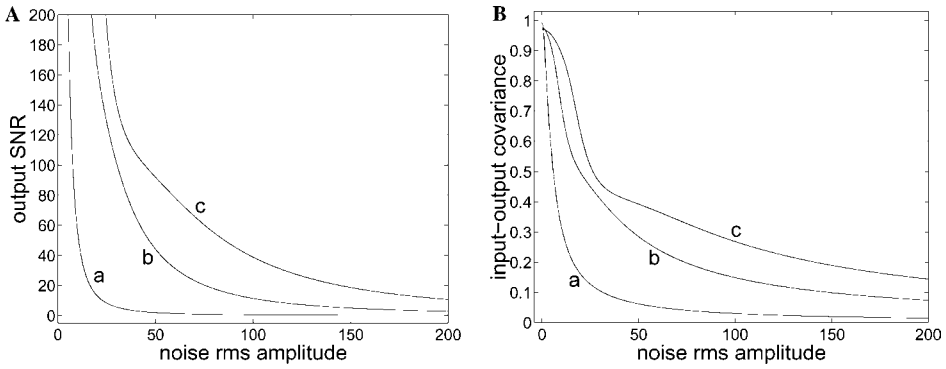


*Figure 3.* Transmission at medium range by the neuron nonlinearity of Equation (1), as a function of the rms amplitude $\sigma_\eta/I_{\text{th}}$ of the zero-mean Gaussian noise $\eta(t)$ with $I_1 = I_0/2$ and (a) $I_0 = 10I_{\text{th}}$ (b) $I_0 = 50I_{\text{th}}$ and (c) $I_0 = 100I_{\text{th}}$. Panel A: Output signal-to-noise ratio $\mathcal{R}_1$ from Equation (8) for the $T_s$-periodic input $s(t)$ of Equation (13). Panel B: Input–output normalized cross-covariance $C_{sf}$ of Equation (12) for the aperiodic input $s(t)$ of Equation (14).

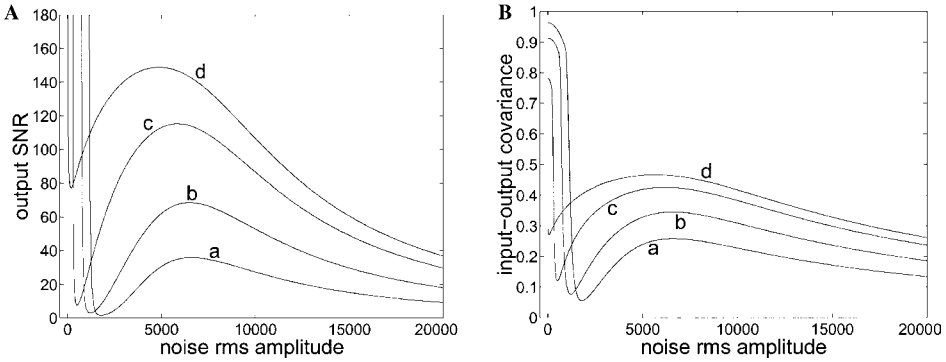


*Figure 4.* Transmission at saturation by the neuron nonlinearity of Equation (1), as a function of the rms amplitude $\sigma_\eta/I_{\text{th}}$ of the zero-mean Gaussian noise $\eta(t)$, with $I_0 = 10^4 I_{\text{th}}$ and (a) $I_1 = 5 \times 10^3 I_{\text{th}}$, (b) $I_1 = 7 \times 10^3 I_{\text{th}}$, (c) $I_1 = 9 \times 10^3 I_{\text{th}}$ and (d) $I_1 = 10^4 I_{\text{th}}$. Panel A: Output signal-to-noise ratio $\mathcal{R}_1$ from Equation (8) for the $T_s$-periodic input $s(t)$ of Equation (13). Panel B: Input–output normalized cross-covariance $C_{sf}$ of Equation (12) for the aperiodic input $s(t)$ of Equation (14).

generally enables complete signal transmission, as measured by $\mathcal{R}_1$ and $C_{sf}$, at zero noise. This translates into an infinite signal-to-noise ratio $\mathcal{R}_1$ in Figure 4A, and a normalized cross-covariance $C_{sf}$ which is close to unity in Figure 4B, when the noise level $\sigma_\eta$ is strictly zero.

Yet, this condition with strictly no noise may not be realistic in practice, and a pre-existing amount of noise is a quite plausible feature. Figure 4 shows that the performance measures $\mathcal{R}_1$ and $C_{sf}$ degrade rapidly when a small amount of noise $\eta(t)$ pre-exists with the coherent input $s(t)$. However, this degradation does not develop monotonically. When more noise is added, a constructive action of the noise is recovered. This is conveyed in Figure 4 by a range of the noise level $\sigma_\eta$ where the performance measures $\mathcal{R}_1$ and $C_{sf}$ improve as $\sigma_\eta$ grows. These nonmonotonic evolutions of the performance in Figure 4, as the noise grows, instead of monotonie degradations, is another form of stochastic resonance, or improvement by noise, in neuronal transmission near saturation this time. When a small amount of noise pre-exists, further addition of noise may bring improvement to the transmission near saturation.

The benefit afforded by the noise is even more pronouced in the case of Figure 4B(d). This is the case of very strong saturation for the transmission of an aperiodic signal assessed by the cross-eovariance $C_{sf}$. In this case, Figure 4B(d) shows that, because of the strong saturation, the performance measured by $C_{sf}$ is rather poor at zero noise. Moreover, at the optimum nonzero noise level, the performance $C_{sf}$ is striclty better than its value at zero noise.

A qualitative explanation for the benefits in Figure 4, is that the added noise, on average, has the ability to pull the neuron response out of the saturation region, back into its curvilinear part, more favorable to an efficient signal transmission. This is a mode of operation of the added noise, which is symmetrical in some sense, with its action in the threshold region. The common feature is that the added noise has the

ability, on average, to shift the operating zone of the neuron nonlinearity into a region more favorable to the signal transmission, avoiding both the threshold and the saturation regions. The phenomenon of stochastic resonance was known to occur in neuronal transmission in the threshold region, but its feasibility in the saturation region as demonstrated here is a novel feature.

## 5. Discussion

We have demonstrated a novel form of stochastic resonance, or noise-aided signal transmission, in the saturation region of a nonlinear neuronal response, where addition of noise can reduce the distortion of large signals in their transduction. This novel form of stochastic resonance complements the other form which was known to occur in the threshold region of the neuronal response. Both forms of stochastic resonance, at threshold and at saturation, were shown feasible here in the same model of neuronal signal transduction. Our results therefore also establish the possibility of broadening the dynamic range of operation of a neuron, from both ends, at threshold for small inputs and at saturation for large inputs, thanks to addition of noise.

Another vision which summarizes the beneficial action of the noise can be obtained if we consider that the input current of Equation (2) is realized as $I(t) = s + \eta(t)$ where $s$ is a constant value. We then measure the output firing rate with the statistical average $\mathrm{E}(f)$ as it results from Equation (6) with a constant input $s$. The noise $\eta(t)$ is added as a zero-mean Gaussian noise whose rms amplitude $\sigma_\eta$ is varied according to

$$\sigma_\eta = I_s \ln(1 + s/I_s). \tag{15}$$

Figures 2 and 4 reveal that the optimal level of noise that maximizes the transmission efficacy will take a precise value whose detail depends on the choice of the measure of performance and on the input signal $s(t)$, but that in general its order of magnitude will be comparable, or slightly below, the level of the information-carrying input. Accordingly, Equation (15) is an empirical law which aims at controlling that the amount $\sigma_\eta$ of the noise is at a level comparable to, or slightly below, that of the information-carrying input $s$. When $s$ in Equation (15) is significantly below the current parameter $I_s$ then $\sigma_\eta$ grows linearly with $s$, and when $s$ is above $I_s$ then $\sigma_\eta$ grows logarithmically with $s$. With added noise injected according to Equation (15), Figure 5 represents the input–output relationship of the output rate $\mathrm{E}(f)$ versus the input current $s$.

Figure 5 shows that the noise realizes a 'softening' of the input–output neuron characteristic, both in the region of the threshold and in the region of the saturation, compared to the noiseless characteristic of Figure 1. Another law comparable to Equation (15) for varying the noise would lead to another softened input–output characteristic for the neuron, but showing qualitatively a comparable effect of the noise. It is to note that the softened characteristics of Figure 5 are not to be taken as

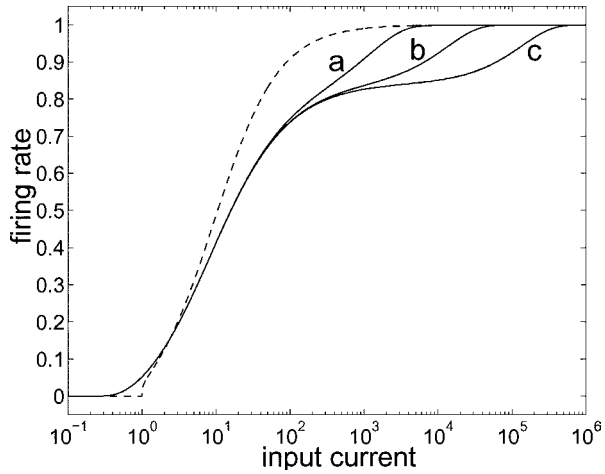


*Figure 5.* Output firing rate in units of $f_{\max} = 1/T_r$, as a function of the input current in units of $I_{th}$. Dotted line: noiseless input–output relationship of Figure 1. Solid lines: input–output relationship with zero-mean Gaussian noise $\eta(t)$ of rms amplitude $\sigma_\eta$ according to Equation (15) with $I_s = 10^3 I_{th}$ (a), $I_s = 10^4 I_{th}$ (b), and $I_s = 10^5 I_{th}$ (c).

the ultimate expression of the possibilities of improvement brought in by the noise, but merely as one possible expression in given conditions. The curves of Figure 5 essentially characterize the transmission of a static, constant, stimulus, with a performance visually assessed by the softened aspect of the characteristics in Figure 5. By contrast, Figure 2–4 characterize the transmission of dynamic, or time-varying inputs, with a performance quantitatively assessed by a signal-to-noise ratio or a cross-covariance measure, meaningful in this context. This picture is in fact consistent with the current status of stochastic resonance: there is no unique way of characterizing the benefit of noise in stochastic resonance. It depends on the type of signal to be transmitted as well as on the type of measure of performance which is selected as meaningful. The common qualitative feature is an improvement brought to a signal by the noise, but the quantitative assessment of the improvement can take various forms, depending on the context.

For the present demonstration of stochastic resonance in neural transmission at threshold and at saturation, it should be noted that the conditions tested here for the coherent input signal $s(t)$ and for the noise $\eta(t)$ (Gaussian), are merely illustrative. The stochastic resonance at saturation, and also at threshold, are robustly preserved in many other configurations for $s(t)$ and $\eta(t)$. These can be investigated in more detail with the exposed methodology.

The present demonstration of a novel form of stochastic resonance for neurons, is based here on the simple model of neuronal signal transduction expressed by Equation (1). As it has been pointed out in many other neuronal studies [10], this model of Equation (1), although realizing a very simplified representation of the neuron dynamics, is able to provide a useful description, at least qualitatively, of important neuron properties. The model of Equation (1) conveys the key features of

the neuronal response that are formed by the threshold and the saturation. These two features are the essential ingredients that allow the various forms of stochastic resonance studied here to take place. The stochastic resonance of Figure 2 which we have observed here with Equation (1) at threshold, has also been verified to exist in more elaborate neuron models [2, 3, 13, 16–18] and also in experiments [5, 6, 8, 19]. In analogy, it is likely that the novel form of stochastic resonance at saturation, whose feasibility in the neuron is reported here for the first time by means of Equation (1), will be qualitatively preserved in more elaborate conditions.

For instance, with more elaborate neuron models taking into account the dynamics of individual spikes, it has been shown in [16, 17] that stochastic resonance occurs for transmission at threshold, confirming in some sense the results of Figure 2. The mechanism is that coherent input spikes which are too rare or not sufficiently active to trigger a response, can receive assistance from a homogenous random excitatory activity from the noise. In a similar way for transmission at saturation, it can be expected that coherent input spikes which would be too numerous or overactive so that they saturate the response, could be mitigated by a homogenous random inhibitory activity from the noise. Another recent study in [20] also describes the output neuron activity with spikes, in an integrate-and-fire model with refractory period, and shows noise-induced resonance effects. These effects are assessed in [20] with statistical measures quantifying the coherence or incoherence of the spiking activity, in place of the signal-to-noise ratio of Equation (8) or the cross-covariance of Equation (12) that we use here. Noise-induced resonances are shown in [20] both in small- and large-noise conditions, as also explored here, although large time-varying information-carrying signals operating the neuron at saturation are not explicitly considered in [20] for reduction of their distortion by addition of noise.

Such types of studies with more elaborate neuron models represent an open perspective useful to complement the report of the feasibility of stochastic resonance at neuron saturation we have presented here. Another open perspective, to parallel the case of stochastic resonance at threshold, is to look for evidence of stochastic resonance at saturation in neuronal experiments.

## References

1. Gammaitoni, L., Hänggi, P., Jung, P. and Marchesoni, F.: Stochastic resonance, *Reviews of Modern Physics*, **70** (1998), 223–287.
2. Bulsara, A., Jacobs, E. W., Zhou, T., Moss, F. and Kiss, L.: Stochastic resonance in a single neuron model: Theory and analog simulation, *Journal of Theoretical Biology*, **152** (1991), 531–555.
3. Longtin, A.: Stochastic resonance in neuron models. *Journal of Statistical Physics*, **70** (1993), 309–327.
4. Sakumura, Y. and Aihara, K.: Stochastic resonance and coincidence detection in single neurons, *Neural Processing Letters*, **16** (2002), 235–242.
5. Douglass, J. K., Wilkens, L., Pantazelou, E. and Moss, F.: Noise enhancement of information transfer in crayfish mechanoreceptors by stochastic resonance, *Nature*, **365** (1993), 337–340.

6. Collins, J. J., Imhoff, T. T. and Grigg, P.: Noise-enhanced information transmission in rat SA1 cutaneous mechanoreceptors via aperiodic stochastic resonance, *Journal of Neurophysiology*, **76** (1996), 642–645.
7. Stacey, W. C. and Durand, D. M.: Stochastic resonance improves signal detection in hippocampal CA1 neurons, *Journal of Neurophysioloyy*, **83** (2000), 1394–1402.
8. Moss, F., Ward, L. M. and Sannita, W. G.: Stochastic resonance and sensory information processing: A tutorial and a review of application, *Clinical Neurophysiology*, **115** (2004), 267–281.
9. Rousseau, D., Rojas Varela, J. and Chapeau-Blondeau, F.: Stochastic resonance for nonlinear sensors with saturation, *Physical Review E*, **67** (021102) (2003), 1–6.
10. Koch, C.: *Biophysics of Computation: Information Processing in Single Neurons*. New York: Oxford University Press, 1999.
11. Chapeau-Blondeau, F. and Chauvet, G.: Dynamic properties of a biologically motivated neural network model, *International Journal of Neural Systems*, **3** (1992), 371–378.
12. Chapeau-Blondeau, F. and Godivier, X.: Theory of stochastic resonance in signal transmission by static nonlinear systems, *Physical Review E*, **55** (1997), 1478–1495.
13. Collins, J. J., Chow, C. C. and Imhoff, T. T.: Aperiodic stochastic resonance in excitable systems, *Physical Review E*, **52** (1995), R3321–R3324.
14. Chapeau-Blondeau, F. and Rojas-Varela, J.: Nonlinear signal propagation enhanced by noise via stochastic resonance, *International Journal of Bifurcation and Chaos*, **10** (2000), 1951–1959.
15. Collins, J. J., Chow, C. C., Capela, A. C. and Imhoff, T. T.: Aperiodic stochastic resonance, *Physical Review E*, **54** (1996), 5575–5584.
16. Chapeau-Blondeau, F., Godivier, X. and Chambet, N.: Stochastic resonance in a neuron model that transmits spike trains, *Physical Review E*, **53**: (1996), 1273–1275.
17. Godivier, X. and Chapeau-Blondeau, F.: Noise-enhanced transmission of spike trains in the neuron, *Europhysics Letters*, **35** (1996), 473–477.
18. Lee, S. G. and Kim, S.: Parameter dependene of stochastic resonance in the stochastic Hodgkin-Huxley neuron, *Physical Review E*, **60** (1999), 826–880.
19. Levin, J. E. and Miller, J. P.: Broadband neural encoding in the cricket cercal sensory system enhanced by stochastic resonance, *Nature*, **380** (1996), 165–168.
20. Lindner, B., Schimansky-Geier, L. and Longtin. A.: Maximizing spike train coherence or incoherence in the leaky integrate-and-fire model, *Physical Review E*, **66**: (031916)(2002), 1–6.